other authors we favor the ion relay mechanism.[24]

Acknowledgment. This research was supported by DOE through Grants FG02-86ER13640 and DEFG02-89ER45220. Facilities of the NSF-DMR sponsored Northwestern University Materials Research Center were used extensively in this research. We thank Dr. Stephen Harper of Arco Chemicals for samples of PPO. We also thank Dr. Kate Doan, Dr. Michael Lerner, Dr. Leslie Lyons, and Professor Mark Ratner for helpful discussions.

Registry No. PPO, 25322-69-4; NaI, 7681-82-5; I_2, 7553-56-2.

Second Harmonic Generation by the Self-Aggregation of Organic Guests in Molecular Sieve Hosts

Sherman D. Cox,† Thurman E. Gier, and Galen D. Stucky*

Department of Chemistry, University of California at Santa Barbara, Santa Barbara, California 93106

Received March 22, 1990

Inclusion of polar organic molecules in molecular sieve hosts has been investigated as a means of creating self-assembled aggregates of molecules that possess the noncentrosymmetry required for materials to exhibit second harmonic generation (SHG). Aluminophosphate molecular sieves with one-dimensional channel structures are shown by SHG powder measurements to successfully direct this self-aggregation for a number of organic molecules including and related to *p*-nitroaniline. Models supported by FTIR evidence show the aggregates could be chains of molecules with a large net dipole that form within the molecular sieve channels. The polar host crystal then aligns the aggregates to produce a large bulk dipole moment and the observed SHG signal. Three methods for controlling the SHG intensity within a particular host structure have been elucidated: (1) variation of guest concentration, (2) alteration of guest structure, and (3) changing the charge density on the host framework.

Introduction

Nonlinear optical properties are determined by the bulk hyperpolarizability tensor, $\chi^{(n)}$, a quantity that, in the second-order case, $\chi^{(2)}$, is very sensitive to symmetry restrictions.[1] For a material to exhibit second harmonic generation (SHG) it must have a noncentrosymmetric component. This single restriction dominates any search for new materials for SHG applications. In solid-state inorganic chemistry the search is for families of compositional types with acentric crystal structures, the KTP family, for example.[2] In molecular chemistry the effort is to align molecules so that a net bulk dipole results. This has been accomplished in crystals by using a variety of strategies[1,3] including the use of molecular asymmetry, chirality, hydrogen bonding, dipole reduction, changing counterions in organic or organometallic salts,[4] and making use of noncentrosymmetric rarrangements in centrosymmetric organic crystals.[5] Dipole alignment in poled polymer, sol gel,[6] and Langmuir–Blodgett films is receiving considerable attention because of device applications.[1]

Inclusion chemistry can accomplish optimization of molecular alignment by careful size and shape matching of host and guest. The first reports of inclusion chemistry as a method of generating nonlinear optical materials, were in 1984, by Tomaru et al.[7] They showed that *p*-nitroaniline and closely related organic guests exhibited SHG 4 times that of urea in the presence of β-cyclodextrin. Wang and Eaton demonstrated shortly thereafter that this was indeed due to inclusion[8] and expanded the field[9] to other hosts (thiourea, tris(*o*-thymotide), and deoxycholic acid) and organometallic guests, mainly of the arylmetal tricarbonyl type.

This work[10] is the first to use crystalline inorganic hosts with organic guests. Inorganic hosts appropriate for consideration in nonlinear optical applications include the molecular sieves and layered materials. Host materials

†Present address: Pfizer Inc., Specialty Minerals, 9 Highland Ave., Bethlehem, PA 18017.

(1) (a) Williams, D. J. *Angew. Chem., Int. Ed. Engl.* **1984**, *23*, 690–703. (b) Hann, R. A., Bloor, D.; Eds. *Royal Society of Chemistry Special Publication No. 69: Organic Materials for Nonlinear Optics. The Proceedings of a Conference Organized by the Applied Solid State Chemistry Group of the Dalton Division of The Royal Society of Chemistry, Oxford, 29th-30th June, 1988*; Royal Society of Chemistry: London, UK, 1989. (c) Khanarian, G., Ed. *Proc. SPIE—Int. Soc. Opt. Eng., Nonlinear Optical Properties of Organic Materials*; SPIE: Bellingham, WA, 1988; Vol. 971. (d) Heeger, A. J., Orenstein, J., Ulrich, D. R., Eds. *MRS Symp. Proc., Nonlinear Optical Properties of Polymers*; MRS: Pittsburgh, PA, 1988; Vol. 109. (e) Chemla, D. S., Zyss, J.; Eds. *Nonlinear Optical Properties of Organic Molecules and Crystals*; Academic Press: New York, 1987; Vol. 1.

(2) (a) Gier, T. E. U.S. Patent No. 4,231,838, 1980. (b) Bierlein, J. D.; Gier, T. E. U.S. Patent No. 3,949,323, 1976. (c) Gier, T. E. U.S. Patent No. 4,305,778, 1981. (d) Bierlein, J. D.; Ferretti, A.; Brixne, L. H.; Hsu, W. H. *Appl. Phys. Lett.* **1987**, *50*, 1216. (e) Eddy, M. M.; Gier, T. E.; Keder, N. L.; Cox, D. E.; Bierlein, J. D.; Jones, G.; Stucky, G. D. *Inorg. Chem.* **1988**, *27*, 1856–1858. (f) Stucky, G. D.; Phillips, M. L. F.; Gier, T. E. *Chem. Mater.* **1989**, *1*, 492–509.

(3) Meredith, G. R. *M.R.S. Bull.* **1988**, *13*(8), 24–29.

(4) Marder, S. R.; Perry, J. W.; Schaefer, W. P. *Science* **1989**, *245*, 626–628.

(5) Weissbuch, I.; Lahav, M.; Leiserowitz, L.; Meredith, G. R.; Vanherzeele, H. *Chem. Mater.* **1989**, *1*, 114–118.

(6) Zink, J. I.; Kaner, R. B.; Dunn, B., private communication.

(7) (a) Tomaru, S.; Zembutsu, S.; Kawachi, M.; Kobayashi, M. *J. Inclusion Phenom.* **1984**, *2*, 885–890. (b) Tomaru, S.; Zembutsu, S.; Kawachi, M.; Kobayashi, M. *J. Chem. Soc., Chem. Commun.* **1984**, 1207–1208.

(8) Wang, Y.; Eaton, D. F. *Chem. Phys. Lett.* **1985**, *120*, 441–444.

(9) (a) Eaton, D. F.; Anderson, A. G.; Tam, W.; Wang, Y. *J. Am. Chem. Soc.* **1987**, *109*, 1886–1888. (b) Tam, W.; Eaton, D. F.; Calabrese, J. C.; Williams, I. D.; Wang, Y.; Anderson, A. G. *Chem. Mater.* **1989**, *1*, 128–140.

(10) Preliminary results have been published: (a) Cox, S. D.; Gier, T. E.; Stucky, G. D.; Bierlein, J. *J. Am. Chem. Soc.* **1988**, *110*, 2986–2987. (b) Cox, S. D.; Gier, T. E.; Stucky, G. D.; Bierlein, J. *Solid State Ionics* **1989**, *32/33*, 513–520.

0897-4756/90/2802-0609$02.50/0

must be transparent in at least part of the optical region (UV to IR) and must be available in a form usable in optical devices, normally thin films or single crystals. Molecular sieves are difficult to obtain as large single crystals, but progress is being made, especially with technologically important materials. Numerous reports have appeared on ZSM-5 (an important petroleum cracking catalyst) crystals in the 0.1–0.8-mm range,[11] for instance. Thin films containing embedded molecular sieves have been reported recently,[12] so that approach is also available. A third approach is via layered inorganic materials, which often have inherent film-forming properties[13] due to their lamellar structure.

The wide variety of pore structure, size, shape, and framework charge density available in the molecular sieves makes them attractive. Size and shape variability allows the host to be matched to the guest so that a chosen orientation in the host pore can be achieved. In this regard one-dimensional polar pore structures are particularly promising for the alignment processes required for SHG. Variation in host framework charge density or dielectric constant, via Si/Al ratio changes, or the use of other framework atoms[14] can be used to define guest–host and guest–guest electrostatic interactions. For example, guest dipole molecules may interact more strongly with one another in a low charge density host than in a high charge density host where guest–host interactions should dominate. In a few low charge density hosts, guest aggregation or chain formation should occur and lead to bulk dipole alignment. The counterions present in the host can also be used to control guest aggregation. Changing the size of the ions alters the pore size and shape and the local electrostatic fields around the ions.

Inorganic hosts have the advantages of rigidity as well as thermal and chemical stability over organic hosts. With a more rigid inorganic host, guest orientation may be amenable to computer simulation using a simple rigid-body host–guest interaction. The thermal stability of organic systems is inherently low because of their molecular nature, whereas inorganic hosts are rugged framework systems stable to several hundered degrees. Some of this thermal stability will be conferred upon the guest through limitations on motional degrees of freedom within the restricted pore space. Rigid inorganic hosts also allow complete variation in guest concentration between empty and filled pores. This range of concentrations provides a simple method to control guest aggregation and bulk nonlinear optic properties.

Host symmetry may be important for the production of SHG. Guest molecules in a centrosymmetric host can cause a structural rearrangement in the host to give a noncentrosymmetric inclusion material[5] that could produce SHG. The centrosymmetric hosts Y, ZSM-5, mordenite,

Chart I

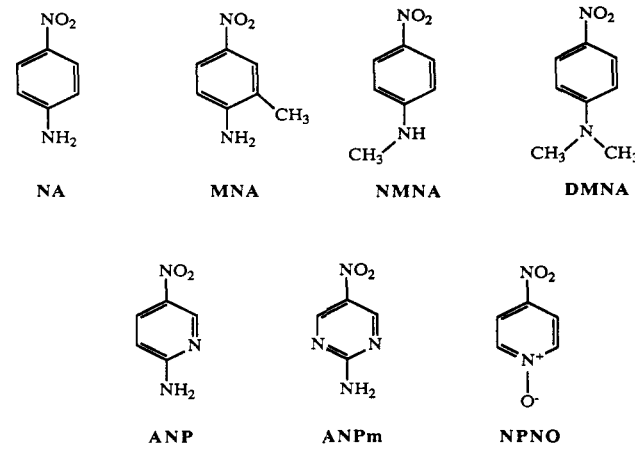

L, and omega were investigated. They provide a good cross section of large-pore zeolite structure types that are available. Zeolite Y is the aluminosilicate with the largest known pore volume. It has a three-dimensional pore system consisting of 13-Å-diameter "supercages" interconnected in a diamondlike lattice through 8-Å-diameter circular 12-ring (composed of 12 tetrahedral atoms linked by bridging oxygens) windows.[15] ZSM-5 is a high silica zeolite that has a three-dimensional channel system consisting of straight 5.4 × 5.6 Å 10-ring channels in one direction and sinusoidal 5.1 × 5.4 Å 10-ring channels perpendicular to the first.[16] Mordenite is an aluminosilicate with a two-dimensional channel system with large 6.7 × 7 Å 12-ring channels interconnected by small 2.9 × 5.7 Å 8-ring openings.[15] L and omega are aluminosilicates that have straight, circular, nonintersecting 12-ring channels with diameters of 7.1 and 7.5 Å, respectively.[15]

A noncentrosymmetric host, on the other hand, could cause guest molecules that normally crystallize in a centrosymmetric fashion to assume the lower symmetry of the host. Noncentrosymmetric molecular sieves include ALPO-5[17] (space group $P6cc$), ALPO-11[18] ($Ic2m$), VPI-5[19] ($P6_3cm$), sodalite[20] ($P\bar{4}3n$), and Offretite[21] ($P\bar{6}m2$). Sodalite has small six-ring openings that are not large enough to allow inclusion of organics after its aluminosilicate framework has formed, although it can be used to clathrate small organic molecules during framework synthesis and for semiconductor inclusion.[22] The other four noncentrosymmetric structures were investigated. They are all one-dimensional channel structures. Offretite is an aluminosilicate with 6.9-Å diameter 12-ring channels. ALPO-5, ALPO-11, and VPI-5 are aluminophosphates with neutral, relatively hydrophobic frameworks. ALPO-11 has elliptical 6.7 × 4.4 Å 10-ring channels, while ALPO-5 and VPI-5 have circular 12-ring and 18-ring channels that are 8 and 12–13 Å in diameter, respectively. Framework substitution of aluminum or phosphorus for silicon (to

(11) (a) Lermer, H.; Draeger, M.; Steffen, J.; Unger, K. K. *Zeolites* **1985**, *5*, 131–134. (b) Guth, J. L.; Kessler, H.; Wey, R. In *Studies in Surface Science and Catalysis*; 7th International Zeolite Conference; Murakami, Y., Iijima, A., Ward, J. W., Eds.; Elsevier: Amsterdam, 1986; Vol. 28, pp 121–128. (c) Hayhurst, D. T.; Lee, J. C. *Ibid.*; pp 113–120. (d) Muller, U.; Unger, K. K. *Zeolites* **1988**, *8*, 154–156.

(12) (a) Bein, T.; Brown, K.; Enzel, P.; Brinker, C. J. *Better Ceramics Through Chemistry III. Mater. Res. Soc. Symp. Proc.* **1988**, *121*, 761–766. (b) Bein, T.; Brown, K.; Brinker, C. J. *Zeolites: Facts, Figures, Future. Stud. Surf. Sci. Catal.* **1989**, *49*, 887–896.

(13) (a) Walker, G. F.; Garrett, W. G. *Science* **1967**, *156*, 385–387. (b) Ballard, D. G. H.; Rideal, G. R. *J. Mater. Sci.* **1983**, *18*, 545–561. (c) Ballard, D. G. H. *Chem. Brit.* **1984**, 538–543.

(14) (a) Bedard, R. L.; Wilson, S. T.; Vail, L. D.; Bennet, J. M.; Flanigen, E. M. Zeolites: Facts, Figures, Future. *Stud. Surf. Sci. Catal.* **1989**, *49*, 375–387. (b) Moran, K. L.; Harrison, W. T. A.; Gier, T. E.; Mac Dougall, J. E.; Stucky, G. D. Materials Research Symposium, Boston, in press.

(15) Breck, D. W. *Zeolite Molecular Sieves*; Wiley: New York, 1974.

(16) Olson, D. H.; Kokotailo, G. T.; Lawton, S. L.; Meier, W. M. *J. Phys. Chem.* **1981**, *85*, 2238–2243.

(17) Bennet, J. M.; Cohen, J. P.; Flanigen, E. M.; Pluth, J. J.; Smith, J. V. In *Intrazeolite Chemistry*; ACS Symposium Series 218, Stucky, G. D., Dwyer, F. G., Eds.; American Chemical Society: Washington, DC, 1983; pp 109–118.

(18) Bennett, J. M.; Richardson, J. W., Jr.; Pluth, J. J.; Smith, J. V. *Zeolites* **1987**, *7*, 160–162.

(19) (a) Davis, M. E.; Saldarriaga, C.; Montes, C.; Garces, J.; Crowder, C. *Nature* **1988**, *331*, 698–699. (b) Davis, M. E.; Saldarriaga, C.; Montes, C.; Garces, J.; Crowder, C. *Zeolites* **1988**, *8*, 362–366.

(20) Felsche, J.; Luger, S.; Baerlocher, Ch. *Zeolites* **1986**, *6*, 367–372.

(21) Gard, J.A.; Tait, J. M. *Acta Crystallogr.* **1972**, *B28*, 825–834.

(22) Stucky, G. D.; Mac Dougall, J. E. *Science* **1990**, *247*, 669–678.

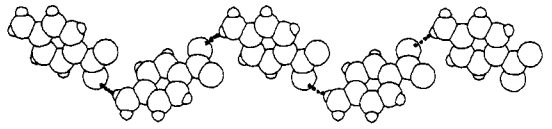

Figure 1. Chain of *p*-nitroaniline molecules as it occurs in the *p*-nitroaniline crystal structure. Hydrogen bonds are indicated as heavy dashed lines.

make SAPOs) or other metals can be used to vary the framework charge density in these hosts.[23] This has been done in this research with the ALPO-5/SAPO-5 pair.

Beta was also studied because its newly elucidated and complex structure[24] consists of chiral units that could lead to second-order nonlinear optic properties. It has a three-dimensionally interconnected 12-ring pore system. But it is a system with a very high level of structural defects and its chiral units may be in racemic pairs, which would result in overall centrosymmetry, so it is not ideally suited for alignment of guests.

Inclusion guests for SHG are conjugated π-electron molecules with attached donor and acceptor groups (e.g., in *p*-nitroaniline (NA)) that lead to charge-transfer excited states. This enhances second-order nonlinear optical properties because of the large change in dipole moment between ground and excited states.[25] Size and shape can be varied by alkylation at the nitrogen atom or on the aromatic ring leaving the electronic system unaffected. Cutoff wavelengths can be shifted into the UV by using pyridine or pyrimidine for the aromatic substrate or toward the red with stilbene or related extended conjugated systems. All of these guest variations have been investigated in this work through use of the organic guests shown in Chart I and others detailed below. Organometallic guests that showed promise in the organic inclusion systems of Eaton et al.[8,9] were also studied.

Only a few organics with favorable molecular nonlinear optical properties have the required noncentrosymmetric structure to show an SHG signal. This is because large dipole molecules such as these have a strong tendency to pair up with dipoles pointed in opposite directions. 2-Methyl-4-nitroaniline (MNA) is a well-known example where this tendency has been overcome. It has the largest single-crystal electrooptic coefficient ($(67 \pm 25) \times 10^{-12}$ m/V)[26] yet measured, and single-crystal SHG measurements showed a harmonic intensity 1.3×10^6 times a quartz reference.[27] NA has the same molecular hyperpolarizability as MNA but crystallizes in a centrosymmetric fashion[28] so that it cannot have any SHG. If NA were properly aligned in a solid, it could have the same nonlinear optic properties as MNA. Comparison between guests that show SHG as pure organics and those that do not is useful in these studies because an organic guest with no SHG that is present as crystals outside the host pores would not affect the observed SHG, whereas very small amounts of MNA, for example, would create a large SHG signal.

Hydrogen bonding plays an important role in determining molecular orientation in many organic crystals of interest for SHG.[29] A particularly ubiquitous molecular arrangement is a chain of molecules with their dipoles pointing all in the same direction as shown in Figure 1. In many structures, such as NA, these chains are present, but the net dipole is zero because equal numbers of chains point in opposite directions. If this mode of aggregation is maintained in an inclusion complex, the possibility of favorable bulk alignment is obvious as long as neighboring chains do not cancel the effect. Hydrogen bonding of guest hydrogens to host framework oxygens supplies another mechanism for controlling guest aggregation and alignment.

In this paper, results will be presented that show that certain inorganic host–organic guest combinations do give rise to guest alignment and aggregation resulting in significant SHG intensities. Spectroscopic and structural characterization aimed at determining the source of these effects will be presented.

Experimental Section

Materials. ALPO-5, ALPO-11, and mordenite (LZM-5) molecular sieves were supplied by Union Carbide Corp. Beta was from Grace. Offretite and L were generous gifts from Dr. D. Corbin of Du Pont. ZSM-5 was supplied by Mobil Corp. SAPO-5[30] and VPI-5[31] were synthesized according to the literature by using Catapal-B hydrated alumina from Vista Chemical, Cab-O-Sil fumed silica, tripropylamine, and dipropylamine from Kodak and 85% phosphoric acid from Fisher Scientific. A VPI-5 sample for use as a standard was supplied by Prof. M. E. Davis of Virginia Polytechnic Institute. Omega[32] and Y[33] were synthesized according to the literature by using Ludox LS colloidal silica from Du Pont, aluminum hydroxide and sodium hydroxide from Fisher, and 25% tetramethylammonium hydroxide solution from Alfa.

All molecular sieves except VPI-5 were dried by heating at 600 °C under flowing oxygen for 12 h followed by 300 °C under oil pump vacuum for 3–6 h. VPI-5 decomposed under flowing oxygen or argon and with deep bed (1 cm) vacuum calcination. It required the use of a thin bed (<3 mm, approximately) and vacuum calcination with a 10 °C/h ramp from 75 to 100 °C followed by a 100 °C/h ramp to 300 °C and a 4-h hold.

p-Nitroaniline (NA), N-methyl-*p*-nitroaniline (NMNA) and *N*,*N*-dimethyl-*p*-nitroaniline (DMNA) were from Kodak. 2-Methyl-4-nitroaniline (MNA) was from Lancaster Synthesis Ltd. 2-Amino-4-nitropyridine (ANP), 2-Amino-4-nitropyrimidine (ANPm), 4-nitropyridine *N*-oxide (NPNO), and 4-(dimethylamino)-4′-nitrostilbene (DMANS) were from Aldrich. Benzene chromium tricarbonyl and cyclohexadiene iron tricarbonyl were from Strem Chemicals. Cyclopentadienylmanganese tricarbonyl was provided by Prof. William C. Kaska. *p*-Amino-*p*′-nitrobiphenyl, *p*-amino-*p*′-nitrodiphenylacetylene, *p*-amino-*p*′-nitrodiphenyldiacetylene, and *p*-(methylthio)-*p*′-nitrodiphenyldiacetylene were generous gifts from Drs. Albert E. Stiegman and Seth R. Marder of JPL.[34]

(23) Lok, B. M.; Messina, C. A.; Patton, R. L.; Gajek, R. T.; Cannan, T. R.; Flanigen, E. M. *J. Am. Chem. Soc.* **1984**, *106*, 6092–6093.
(24) (a) Treacy, M. M. J.; Newsam, J. M. *Nature* **1988**, *332*, 249–251. (b) Higgins, J. B.; LaPierre, R. B.; Schlenker, J. L.; Rohrman, A. C.; Wood, D.; Kerr, G. T.; Rohrbaugh, W. J. *Zeolites* **1988**, *8*, 446–452.
(25) Oudar, J. L.; Chemla, D. S. *J. Chem. Phys.* **1977**, *66*, 2664–2668.
(26) Singer, K. D.; Lalama, S. L.; Sohn, J. E.; Small, R. D. In ref 1e, Chapter II-8, pp 437–468.
(27) Levine, B. F.; Bethea, C. G.; Thurmond, C. D.; Lynch, R. T.; Bernstein, J. L. *J. Appl. Phys.* **1979**, *50*, 2523–2527.
(28) Trueblood, K. N.; Goldish, E.; Donohue, J. *Acta. Crystallogr.* **1961**, *14*, 1009–1017.
(29) (a) Etter, M. C.; Frankenbach, G. M. *Chem. Mater.* **1989**, *1*, 10–12. (b) Panunto, T. W.; Urbanczyk-Lipkowska, Z.; Johnson, R.; Etter, M. C. *J. Am. Chem. Soc.* **1987**, *109*, 7786–7797. (c) Etter, M. C. *Isr. J. Chem.* **1985**, *25*, 312–319. (d) Etter, M. C. *J. Am. Chem. Soc.* **1982**, *104*, 1095–1096.
(30) Lok, B. M.; Messina, A.; Patton, R. L.; Gajek, R. T.; Cannan, T. R.; Flanigen, E. M. U.S. Patent 4,440,871, 1984. The procedure outlined in example 1 was followed, but 1 equiv of tripropylamine was used as base and hydrochloric acid was omitted.
(31) Davis, M. E.; Montes, C.; Garces, J. M. *ACS Symp. Ser.* **1989**, *398*, 291–304.
(32) Araya, A.; Barber, T. J.; Lowe, B. M.; Sinclair, D. M.; Varma, A. *Zeolites* **1984**, *4*, 263–269. The conditions specified for run A6 were used except that tetramethylammonium chloride and not bromide was the template.
(33) Used the stoichiometry outlined in ref 15, pp 277–279, and the procedure from: Rollmann, L. D.; Valyocsik, E. W. *Inorg. Synth.* **1983**, *22*, 61–68.
(34) The nonlinear optical properties of this series of organic compounds have been reported: Perry, J. W.; Stiegman, A. E.; Marder, S. R.; Coulter, D. R. In ref 1b, pp 189–195.

NA and MNA were purified by double-vacuum sublimation followed by recrystallization from 95% ethanol. NMNA, DMNA, ANP, and DMANS were purified by vacuum sublimation. The other materials were used as received.

Synthesis. Loading of organics: Samples were prepared by using a vapor-phase loading method. Desired portions of predried molecular sieve and organic were weighed into an ampule fitted with a vacuum stopcock. This step was done in the purified argon atmosphere of a Vacuum Atmospheres glovebox. The stopcock was closed off and connected to a vacuum line, the ampule evacuated to oil pump vacuum, and the stopcock closed off again. The sample was thoroughly mixed and heated to 100 °C overnight. At loadings greater than about 10%, small quantities of organic would sublime into the cooler neck of the ampule. The amount that sublimed was checked in a few cases and found to be insignificant. In the case of high (15–30 wt %) loadings of NA in VPI-5, sealed ampules were used to avoid this problem.

ALPO-5 synthesis with fluoride ion: In a plastic beaker with a Teflon-coated stir bar 3.66 g of Catapal B (25 mmol of Al_2O_3) was suspended in 13.70 g of H_2O. A solution of 5.76 g of 85% H_3PO_4 (25 mmol P_2O_5) in 15.2 g of H_2O (total 1.25 mol of H_2O from all sources, 50 equiv) was added with stirring. The resulting gel was covered and stirred for 2 h. Tripropylamine (4.8 mL 25 mmol of Pr_3N, 1 equiv) was added, and stirring was continued for 2 h. Ammonium bifluoride (NH_4F·HF, from Fisher, 0.075 g, 1.3 mmol, 0.05 equiv) was added, and the mixture stirred 30 min. Then 12.0-g batches of the resulting gel were sealed in 23 mL Parr reaction bombs with Teflon liners, heated to 150 °C for 24 h, and cooled to room temperature over several hours. The mixture was suspended in about 300 mL of H_2O, allowed to settle, and decanted to remove any fine amorphous material. This was repeated three times. The solids were filtered and air dried.

ALPO-5 crystal growth was carried out with some variation from the literature[35] by using tripropylamine as the template and Catapal B as the alumina source. A gel with the composition $1.5Pr_3N:Al_2O_3:P_2O_5:300H_2O$ was heated to 150 °C for 3 days.

Characterization: SHG measurements were made using an apparatus configured as described by Kurtz and Perry,[36] Dougherty and Kurtz,[37] and Velsko.[38] Intensities are reported relative to a quartz reference. The data reported by using a fundamental wavelength of 1.907 μm were obtained at the Jet Propulsion Laboratory under the guidance of Dr. J. Perry and are referenced to urea. The reference was checked after every fourth or fifth sample to compensate for any drift. SHG values for which uncertainties are reported were determined as follows: Samples were loaded into standard melting point capillaries in a glovebox and sealed with parrafin wax. A Kigre MK-367 Nd:YAG laser operating in single-shot mode at approximately 20 mJ/pulse was used to illuminate the sample. A Tektronics 2467B 400 MHz oscilloscope with a Tektronics C1001 video camera was used to transfer pulse shapes to an IBM-compatible computer, where the data was analyzed by using Tektronics DCS01 digitizing camera system software. The ratio of the peak intensities of the SHG channel to the reference channel from 13 laser pulses was averaged for each sample. When the standard deviation of these ratios exceeded 30%, up to two low and two high values were discarded so that a 30% or better level of uncertainty was obtained. The SHG values reported are this ratio divided by a similarly determined ratio for quartz. The uncertainties reported are standard deviations of the raw data and do not account for the additional uncertainty of the quartz measurement or other experimental uncertainties such as particle size.

Velsko et al. have shown that powder SHG data can give reliable results that agree well with single-crystal nonlinear optic characterization[38] when careful attention is paid to sample preparation and signal handling. Molecular sieve samples were chosen with as uniform a size as possible of 1 μm. It should be emphasized that the effect of particle size on SHG is alleviated when comparing organic guests in the same host because they have the same distribution of particle size and crystallite morphology. This is of particular importance for studies with varying guest loading level.

X-ray powder diffraction patterns were obtained on a Scintag PADX θ–θ diffractometer using Cu Kα radiation and associated software running on a Microvax II computer. Samples were run in air to check for crystallinity and unit cell expansion or in some cases in a home-built air-tight cell Kapton window. d spacings were referenced to internal silicon standard.

Infrared spectra were obtained on a Digilab FTS-60 FTIR spectrometer with a Spectra Tech diffuse reflectance attachment and a home-built inert atmosphere cell with KBr windows. Pure samples were loaded into the cell in the purified argon atmosphere of a Vacuum Atmospheres glovebox. Sixty-four scans were taken at a resolution of 8 cm^{-1}.

Ultraviolet–visible spectroscopy was done in diffuse reflectance mode using a Cary 14 spectrophotometer with a 1411 attachment with a magnesium carbonate block in the reference window. Samples diluted to 20–30% in magnesium carbonate were pressed between a quartz window and a Pyrex slide and the sandwich held together with tape. Data were recorded in absorbance mode on the original Cary 14 chart recorder, and no Kubelka-Munk function was applied. Data at wavelengths shorter than 260 nm are unreliable due to instrumental difficulties.

^{31}P magic-angle spinning (MAS) and cross polarization (CP) MAS nuclear magnetic resonance (NMR) spectra were obtained on a General Electric GN-300 spectrometer with a Chemagnetics probe, ca. 3-kHz spinning speed, and 100-μs CP contact time. Chemical shifts were referenced to 85% phosphoric acid.

Thermogravimetric analysis (TGA) and differential scanning calorimetry (DSC) was carried out using a Du Pont 9900 TGA-DSC system. An oil pump vacuum was applied to the TGA module through a flexible hose to minimize vibration. DSC samples were crimp-sealed in air-tight aluminum sample holders in the glovebox to avoid the appearance of a large endotherm due to water loss. A temperature ramp of 10 °C/min from 30 to 300 °C was used for both techniques.

Molecular graphics and modeling were done with CHEM-X, developed and distributed by Chemical Design, Ltd., Oxford, England.

Results and Discussion

Significant SHG signals are produced by the aluminophosphate hosts ALPO-11, ALPO-5, and VPI-5 with a variety of included organics. NA and MNA in ALPO-5 have been most extensively studied and will be discussed in detail below. No guest alignment has been observed in any of the centrosymmetric hosts, offretite, or beta with NA, MNA, NMNA, or NPNO. Although not all host–guest combinations have been tried, these representative samples mean that finding a centrosymmetric host that will produce SHG will not be straightforward. The flip side to this is that the noncentrosymmetry of the aluminophosphates is caused only by the ordering of aluminum and phosphorus atoms[17,18] and would not be present in a pure silica polymorph, for instance. Thus the structural or electronic reasons for guest alignment are subtle, and seemingly minor changes in the host, such as variations in the homogeneity of framework atom distribution, or in the guest might produce surprising results.

NA and MNA in ALPO-5. SHG results: SHG as a function of weight percent loading is shown overlaid with unit cell volume in Figure 2, top, for NA and Figure 2, bottom, for MNA. The unit cell volumes increase regularly with loading in both cases, demonstrating definitively that the organic molecule is located inside the molecular sieve pores. The included organic exerts a greater pressure on the inside of the pores than air or water, which is present in the nominally empty molecular sieve. The highest loading level in each case shows external crystalline organic in the X-ray diffraction pattern. SHG results for NA and

(35) (a) Jahn, E.; Müller, D.; Wieker, W.; Richter-Mendau, J. *Zeolites* **1989**, *9*, 177–181. (b) Qui, S.; Peng, W.; Kessler, H.; Guth, J.-L. *Ibid.* **1989**, *9*, 440–444.

(36) Kurtz, S. K.; Perry, T. T. *J. Appl. Phys.* **1968**, *39*, 3798–3813.

(37) Dougherty, J. P.; Kurtz, S. K. *J. Appl. Crystallogr.* **1976**, *9*, 145–158.

(38) Eimerl, D.; Velsko, S. *Laser Program Annual Report UCRL 50021-85*; **1985**, p 7.69.

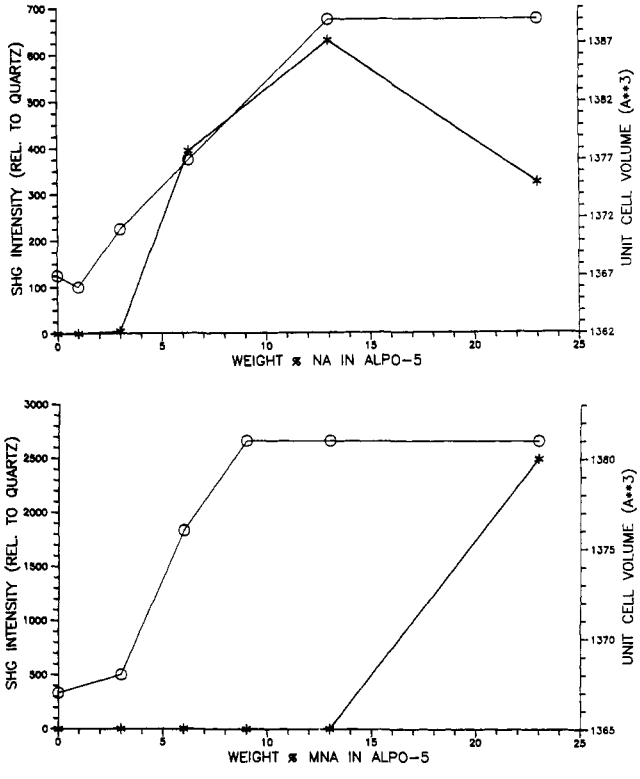

Figure 2. NA (top) and MNA (bottom) in ALPO-5: relative SHG intensity (*) and unit cell volume in Å^3 (O) versus wt % NA (top) and MNA (bottom).

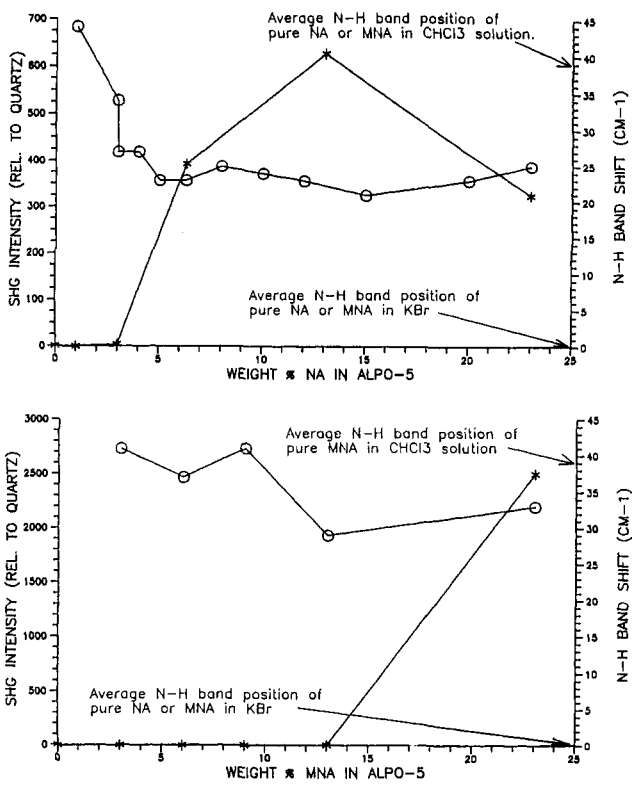

Figure 3. NA (top) and MNA (bottom) in ALPO-5: relative SHG intensity (*) and IR N-H band shift (cm^{-1}) (O) versus weight % NA (top) and MNA (bottom). The N-H band shift is obtained by subtracting the average position of the two major N-H bands in NA (in KBr) from the corresponding average position in the inclusion material.

MNA are strikingly different. NA shows a SHG threshold at around 3%. SHG then rises sharply to a maximum of about 650 at 13% loading. Thus *the SHG of NA is turned on by inclusion into ALPO-5.* MNA in ALPO-5 has no SHG until crystals of MNA are present at the highest loading. The SHG at 13% MNA is less than quartz, about the same as the ALPO-5 host alone. *The SHG of MNA is thus turned off by inclusion.* Since MNA has a single crystal SHG intensity of >10^6 times that of quartz,[27] this shows that at 13% loading *no MNA crystallizes on the external surface of the host.* The other guest molecules used in this study are loaded into the host in a similar fashion, so it is reasonable to assume that interference from external guest crystals is not a problem at loadings below the pore-filling level. This SHG switching of NA and MNA is a dramatic example of how changes in guest size and shape can influence nonlinear optic properties in host–guest systems.

The observation of SHG in samples of NA in ALPO-5 shows in and of itself that ordering and dipole alignment of the NA molecules is occurring. The result that NA is aligned by ALPO-5 was foreseen by the authors of the original structure paper who commented on the polar nature of the crystals: "The concept of polar diffusion should be explored: at low temperature, polar molecules should adopt a specific orientation during diffusion down a polar channel."[17] We propose that the SHG effects are a direct result of the polar properties of ALPO-5 crystals.

The overall increase in SHG with NA loading is due, in part, to the increasing number density of NA molecules present. But the more than 10-fold increase in SHG from 3 to 6% loading cannot be attributed to this alone. Furthermore, if NA molecules were being aligned at the 1% loading level, for instance, a substantial SHG signal would be observed because the molecular hyperpolarizability of NA is so large. Diluting MNA to the 1% level in an inert matrix such as sodium chloride shows this to be the case.

SHG threshold: The SHG threshold phenomenon observed in NA in ALPO-5 could be rationalized in terms of a packing-density argument. At low loadings the guest molecules are independent and can distribute randomly within the pores. At a particular loading threshold, about 3%, the packing density is such that the molecules start to interact and lose their randomness, and the nonlinear effect turns on. The guest molecules may also tend to aggregate at all loading levels, but the argument can proceed in a similar manner. If aggregation occurs at all loadings, guest molecules will see similar chemical environments, a combination of the framework and other guest molecules, at both low and high loadings. If aggregation does not occur at all loadings, at low loadings guest molecules will be exposed only to the framework, so whether or not aggregation occurs could be determined spectroscopically.

FTIR data: To investigate the cause of the SHG threshold, we looked at hydrogen-bonding effects. The crystal structures of NA[28] and MNA[39] both show chains of molecules held together by H bonds between amino hydrogens and nitro oxygens, shown in Figure 1 for NA. A comparison of the IR N–H bands in the pure and the included organic should show if the chain structure has been disturbed by inclusion. NA and MNA in KBr both have N–H stretching bands at about 3480, 3360, and 3230 cm^{-1}. In chloroform two bands appear at 3510 and 3410 cm^{-1}, the higher energies indicating the absence of H bonding. Diffuse reflectance FTIR spectra of NA and MNA in ALPO-5 show two bands at 3510–3500 and 3390–3415 cm^{-1} (intensity is off-scale at high loadings) with

(39) Lipscomb, G. F.; Garito, A. F.; Narang, R. S. *J. Chem. Phys.* **1981**, *75*, 1509–1516.

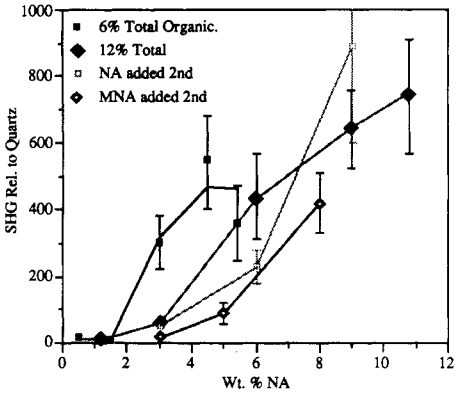

Figure 4. Relative SHG intensity versus wt % NA in mixed systems.

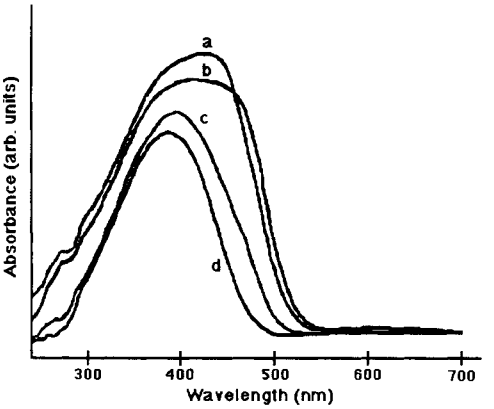

Figure 5. Diffuse reflectance UV–vis spectra of (a) dry 12 wt % NA in ALPO-5, (b) 12 wt % NA in ALPO-5 in air, (c) dry 1 wt % NA in ALPO-5, (d) 1 wt % NA in ALPO-5 in air.

a much weaker band at 3250–3230 cm^{-1}. Obviously, much less H bonding is occurring in the inclusion materials than in the pure organic solids. The difference between the average of the two major N–H bands in the ALPO-5 samples and the average of the corresponding two bands in the pure organics in KBr (3420 cm^{-1}) was used as a quantitative measure of the strength of H bonding. Figure 3, top and bottom, shows the SHG data overlaid with these N–H band shifts for NA and MNA, respectively. There is an obvious parallel trend. For NA at the lowest loading there is a +40-cm^{-1} shift from the pure, solid organic value. NA in chloroform solution has the same N–H band position, so essentially all H bonding is lost. Aggregation does not seem to be occurring at the lowest loading level. This also shows that H-bonding to framework oxygen atoms is not present at the lowest loading and so is probably not a factor in the aluminophosphate host systems. The N–H band position shifts rapidly with increasing loading. A shoulder in one of the bands appears at 3%, indicated by two data points arranged vertically, and is gone by 5%. Just as SHG appears, the N–H band position levels out at an intermediate value. So in samples that show SHG there is weak H-bonding. MNA shows no increase in H-bonding with increasing loading levels, which corresponds to the flat SHG results. The conclusion is that weak intermolecular hydrogen bonding leading to the formation of molecular chains or aggregates plays an important role in SHG production for NA in ALPO-5. The switching off of MNA may be due to an inability to form H-bonds because the added methyl group on MNA restricts its orientation in the ALPO-5 channels.

Mixed NA and MNA studies: Mixing NA and MNA within ALPO-5 pores might provide further evidence for the important influence of intermolecular interactions on the SHG. Would adding a small amount of MNA to a NA sample disrupt the alignment, or conversely would NA in a MNA sample cause alignment of all the molecules to occur? The mobility of the guest molecules could also be probed by comparing the SHG of samples prepared by sequential addition of one guest and then the other with samples prepared by concurrent, random loading. If NA molecules are fairly immobile in ALPO-5, adding additional MNA to an already formed NA/ALPO-5 sample would not change the SHG since MNA is not aligned by ALPO-5. But if there is mobility, the two loading methods should give similar results.

These ideas were investigated at a total NA + MNA loading of 12%, and the results are shown in Figure 4. Also shown is an experiment with concurrent, random loading at 6% total. At 12% total loading, concurrent addition of NA and MNA results in the same pattern as adding only NA (Figure 2, top). No significant alignment of MNA by NA or disordering of NA by MNA seems to be occurring. NA and MNA may segregate into regions or into individual pores that contain only one type of guest molecule. Sequential loading does not provide a clear pattern either. Adding either NA or MNA to samples containing the opposite member of the pair depresses the SHG somewhat, but this difference may not be significant since the uncertainty in these measurements is large. Therefore, at 12% loading NA and MNA appear to act independently with NA molecules forming aligned aggregates as if no MNA were present.

At 6% total loading, alignment of MNA by NA is occurring. At a NA level of only 3%, the SHG corresponds to a 5–6% NA loading, so *MNA is contributing to the SHG.* The difference between 6 and 12% loadings could be due to the extra space available in the host pores at the 6% loading level, which could allow greater conformational freedom for NA and MNA molecules to successfully interact and become aligned. Also, the SHG vs wt % NA curve has a steep slope at the 6% level but is flat at 12%, so small changes in the number of aligned molecules would make a big difference at 6% but not at 12%.

Stability: Exposure to ambient air does not cause displacement of the guest from the ALPO-5 pores according to X-ray powder diffraction, but SHG results show some diminution in air. A 6% NA sample with SHG 0.79 times that of urea (at 1.907 μm) fell to 0.26 times that of urea in air. An 8% NA sample with SHG 800 times that of quartz (at 1.064 μm) fell to 430 times that of quartz in air. These results are attributed to disruption of NA hydrogen bonding by water molecules.

NA and MNA samples in ALPO-5 are all bright yellow, the color being nearly independent of loading. Only at the 1% loading level does the color become noticeably lighter. The color of this sample lightens even further on air exposure. Higher loadings do not lighten in air. Diffuse reflectance UV–vis spectra of 1 and 12% NA/ALPO-5 samples protected from and exposed to the air are shown in Figure 5. At 12% loading exposure to air broadens the band and moves the band edge only slightly, but at 1% the whole band moves noticeably to shorter wavelength. Also, the intensity of the band is not at all proportional to the loading level. Both of these samples were carefully diluted to 33% NA/ALPO-5 with magnesium carbonate, so that there is a 12-fold difference in NA concentration but less than 50% difference in absorbance.

The guest molecules are strongly physisorbed but washing the samples with solvents such as chloroform or acetone does result in extraction of the organic from the

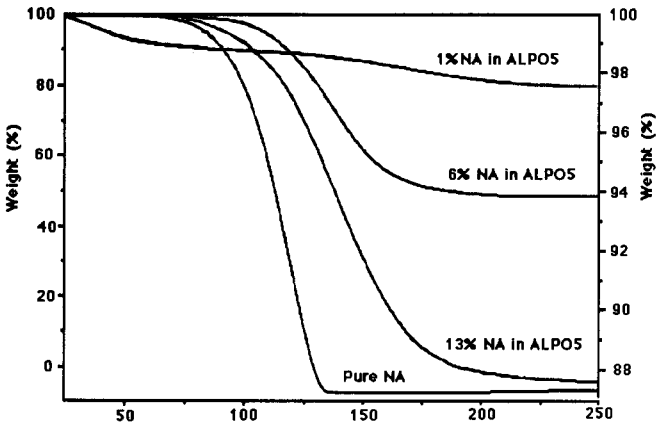

Figure 6. TGA data for pure NA (left-hand y axis) and 13% NA in ALPO-5 (right-hand y axis). Note the steady increase in onset temperature with decreasing NA content.

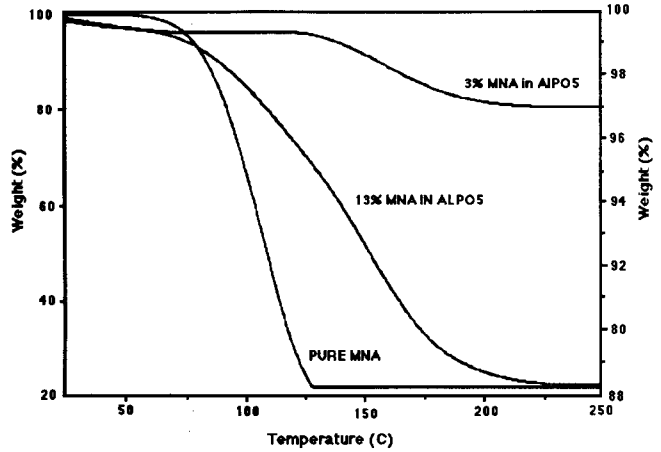

Figure 7. TGA data for pure MNA (left-hand y axis) and 3 and 13% MNA in ALPO-5 (right-hand y axis). Note the low onset temperature of the 13% MNA sample and the two weight-loss regions.

host. Heating to 100°C under dynamic vacuum does not result in any weight loss except when excess organic, not included within the molecular sieve pores, is present. This happens between 15 and 20 percent organic for ALPO-5. Figure 6 shows TGA results for NA in ALPO-5. A single weight loss from 115 to 175 °C is observed for 6–13% NA. Pure NA sublimes at lower temperatures from 85 to 130 °C, under these conditions. At 1% NA the weight loss is at even higher temperatures, 125–200 °C. An important conclusion is that enhanced thermal stability is conferred upon the guest by the host. MNA in ALPO-5 has a key difference, shown in Figure 7. The 13% MNA curve has two fairly straight sections with different slope, indicating that two weight loss processes are occurring. The one at lower temperature appears to coincide with free MNA, but this sample had no SHG so that no free MNA can be present. This implies that there are two types of MNA molecule at the 13% loading level, one more loosely held within the framework than the other. This could be a reflection of the disorder causing the loss of SHG. At lower loadings only one weight loss at higher temperatures is observed, as with NA.

DSC data on NA and MNA in ALPO-5 were taken in hopes of seeing an order–disorder transition. No transitions were seen between 30 and 300 °C except for decomposition at about 210 °C when the samples became black. The lack of any transition may indicate a degree of mobility of the organic that simply increases steadily with temperature or there could be a second-order transition without any significant DSC effect. One run starting at about 0 °C also showed no transition. Lower temperatures could reveal a freezing or ordering temperature but have not been investigated.

NMR studies: MAS and CP-MAS ^{31}P NMR data on NA in ALPO-5 shows a distinct difference between samples with large and small SHG intensities. Cross polarization allows detection of all phosphorus atoms near hydrogen atoms or in any ALPO-5 crystallite that contains a significant number of hydrogen atoms because of dipole coupling between the 100% abundant phosphorus nuclei. In pure, dry ALPO-5 only a very weak signal in the CP spectrum is present as expected, probably due to a hydrogen containing impurity. 3% NA has a signal at −30.25 ppm, and 15% NA has a signal at −30.39 ppm. This shows that the NA hydrogens are close enough to framework phosphorus atoms for cross polarization to occur. Single-pulse spectra showing the total phosphorus signal exhibit a −0.56 ppm shift going from pure ALPO-5 to 15% NA and a change in line shape from a broad, Gaussian shape in pure ALPO-5 and 3% NA to a narrower, Lorentzian shape in 15% NA. Thus 3% NA and pure ALPO-5 have very similar NMR spectra, and both have very low SHG signals.

A correlation between ^{31}P NMR chemical shift and O–P–O bond angle has been elucidated[40] and is found to be −0.51 ppm/deg. The expansion of the unit cell upon loading (observed by X-ray diffraction), which would increase this angle, is probably the source of the chemical shift changes. The correlation given above[40] indicates that the O–P–O angle increases by just over 1° during loading. The change in line shape on loading could be due to a variety of factors, including a change in ^{27}Al quadrupolar coupling to ^{31}P. Additional solid-state studies on selectively deuterated samples to better define the molecular dynamics of these materials are in progress.

Structural data: Without complete structural information, no full explanation of the SHG results is possible. Two sample improvements were made in attempts to increase the quality of available diffraction data. The first was to increase the crystallinity of the host in powder form. This was accomplished by synthesis with added fluoride ion. Fluoride has been shown to aid in the crystallization of aluminosilicates.[41] Attempts at Rietveld refinement[42] using the GSAS program[43] of a sample made with this more crystalline ALPO-5 have so far not yielded a convergent solution. The other sample improvement was the growth of single crystals of up to 300 μm. Variable loading of organic guests in these crystals has been readily accomplished by heating to different temperatures. It is expected that the inorganic host and the organic guest lattices may not be congruent. However, the ordering indicated by the IR and SHG measurements strongly support that both lattices are crystallographic with a long-range order. This conclusion has been recently substantiated by single-crystal data on loaded and unloaded samples. This problem of substantially resolving two noncongruent lattices is not trivial but has been successfully carried out with, for example, one-dimensional organic conductors[44] and is cur-

(40) Müller, D.; Jahn, E.; Ladwig, G.; Haubenreisser, U. *Chem. Phys. Lett.* **1984**, *109*, 332–336.
(41) Guth, J. L.; Kessler, H.; Wey, R. *Stud. Surf. Sci. Catal.* **1986**, *28*, 121–128.
(42) Rietveld, H. M. *J. Appl. Crystallogr.* **1969**, *2*, 65–71.
(43) Larson, A. C.; Von Dreel, R. B. *Generalized Crystal Structure Analysis System, Los Alamos Report LAUR*; 86–748, 1987.
(44) (a) Petricek, V.; Coppens, P.; Becker, P. *Acta Crystallogr.* **1985**, *A41*, 478–483. (b) Gao, Y.; Gajhedt, M.; Mallinson, P.; Petricek, V.; Coppens, P. *Phys. Rev. B* **1988**, *37*, 1824–1831.

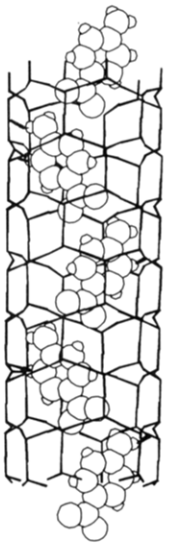

Figure 8. Chain of NA molecules from Figure 1 within a channel of ALPO-5. Short (<2 Å) internuclear contacts are shown as heavy lines. Two of the contacts are less than 1.5 Å.

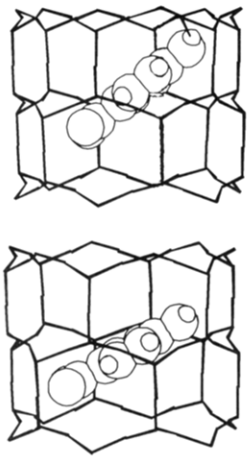

Figure 9. Two possible orientations of the NA molecule in the ALPO-5 channel that have van der Waals distances between host and guest atoms. Internuclear distances are greater than 3 Å for NA nitro oxygens to framework oxygens and greater than about 2 Å for NA amino hydrogens to framework oxygens.

rently being pursued with synchrotron radiation.

Models of guest aggregation: Modeling based on chemical knowledge can be an aid in thinking about possible structures. The IR data presented show that structural fragments present in the pure organic that involve hydrogen bonding are disrupted at least partially in the inclusion complex. This is confirmed by modeling. If a chain of NA molecules (Figure 1) is forced into an ALPO-5 channel, many interatomic distances are less than van der Waals, as shown in Figure 8. This chain would fit easily if stretched or straightened out moderately. Figure 9 shows two orientations of NA with reasonable van der Waals contacts with the ALPO-5 channel. The angle these molecules make with the channel axis is approximately 60°, very close to the optimal angle for maximum SHG, which Oudar and Zyss[45] determined for the ALPO-5 point group (54.74° for 6*mm*).

A simple geometric calculation of the amount of space available within the ALPO-5 pores shows that at 13% NA loading there is 5.3 Å of channel length available for each

(45) (a) Oudar, J. L.; Zyss, J. *Phys. Rev. A* **1982**, *26*, 2016–2027. (b) Zyss, J.; Oudar, J. L. *Phys. Rev. A* **1982**, *26*, 2028–2048.

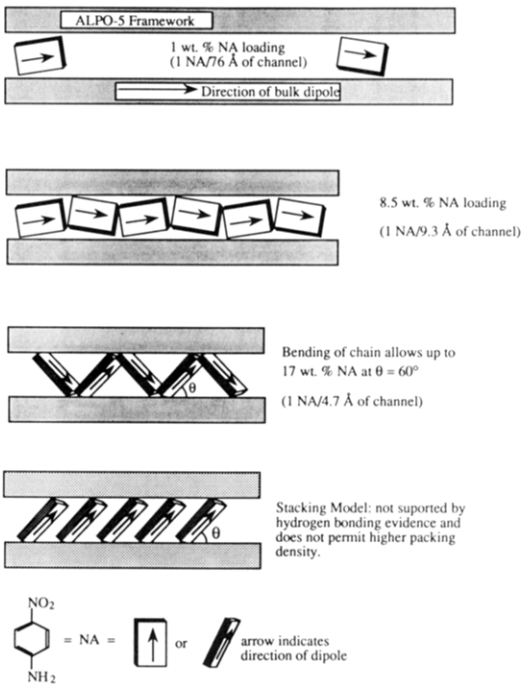

Figure 10. Models for self-aggregation of NA molecules in the ALPO-5 channel.

NA molecule. As a first guess one might assume that the NA molecules would form a stack in the channel as shown at the bottom of Figure 10. With a closest interplanar approach between NA molecules of 3.5 Å, the angle between the channel axis and the molecular plane would be 41° at 13% NA loading. The 60° angle mentioned above is reasonable and would allow a greater interplanar separation.

To fit intermolecular hydrogen bonding into this model, a head-to-tail rather than stacked arrangement must be assumed. This bent chain arrangement is shown second from the bottom in Figure 10. The arrangement of amino and nitro groups results in a bent O–H–N angle, which is very poor for H bonding. The IR data show that H bonding is weak, so that this could be the situation. At lower loadings the molecules could rotate about their long molecular axes as in Figure 9 and in the drawing depicting 8.5% NA loading in Figure 10. The latter drawing shows that a NA chain in the ALPO-5 channel would be a stretched-out version of the chain in the pure organic. This would also reduce H bonding compared to the pure organic. Models show that two NA chains cannot overlap one another in an ALPO-5 channel, so for the maximum observed loading of 15–18 wt % NA to be achieved, the molecules must pack very tightly. The bent chain model predicts that at a maximum angle of 60°, the maximum packing density will be 17 wt %, in agreement with the observed loading limit.

The flattening of SHG above 8–10% may be a reflection of the smaller contribution of each molecule to the total bulk dipole as loading increases. Once a stretched out chain fills a channel, which occurs at 8.5% NA loading in the model, further packing results only in a reduction of the component of each molecular dipole pointing along the channel axis, so that the total bulk dipole cannot increase.

Other Guests. SHG data for other organics and organometallics in ALPO-5 are presented in Table I. NA and ANP are the only molecules tried that have large SHG intensities in ALPO-5. Most surprisingly, *ANPm, with the same size and shape as NA, is not aligned by ALPO-5.* The effect of *N*-methyl substitution was investigated in

Table I

guest[a]	loading, wt %	SHG vs quartz[b] at 1.064 μm	SHG vs urea[c] at 1.907 μm
NA	12	1000 (200)	1.03
MNA	13	0.2 (0.05)	
NMNA	12	50 (10)	0.05
DMNA	12	0.9 (0.3)	0
ANP	12	970 (250)	0.8
ANPm	10	3 (1)	0
NPNO	10	0.5 (0.1)	
DMANS	10		0
$NO_2C_6H_4$–$C_6H_4NH_2$	10		0.2
$NO_2C_6H_4$–CC–$C_6H_4NH_2$	10		0
$NO_2C_6H_4$–CC–CC–$C_6H_4SCH_3$	10		0
cyclohexadiene $Fe(CO)_3$	10		0
benzene $Cr(CO)_3$	12		0
cyclopentadienyl $Mn(CO)_3$	10		0

[a] SHG of pure guests: MNA = 22 times that of urea (from ref 1a), NMNA = 9 times that of quartz, DMNA = 50 times that of quartz, $NO_2C_6H_4$–$C_6H_4NH_2$ = 2 times that of urea (from ref 27), urea = 250 times that of quartz (NMNA, DMNA and urea were measured at UCSB for this work). All other SHG = 0–1 times that of quartz from literature or measured. [b] Data taken at UCSB; uncertainties in parentheses. [c] Data taken at JPL.

Table II[a]

guest	host ALPO-5[b]	SAPO-5[c]	ALPO-11[d]	VPI-5[e]
NA	1000 (200)	280 (70)	500 (130)	50 (10)
MNA	0.2 (0.05)	0.7 (0.2)	120 (30)	90 (20)
NMNA	50 (10)	8 (3)	37 (10)	40 (9)
DMNA	0.9 (0.3)	0.4 (0.1)	110 (50)	15 (3)
ANP	970 (250)	500 (50)	140 (40)	150 (30)
ANPm	3 (1)	1.1 (0.3)	55 (10)	70 (20)
NPNO	0.5 (0.1)	0.5 (0.1)	6 (1)	33 (5)

[a] SHG data relative to quartz; uncertainties shown in parentheses. [b] 10–13 wt % guest loading level. [c] 12 wt % guest loading level. [d] 9–10 wt % guest loading level. [e] 20 wt % guest loading level.

the series NA, NMNA, and DMNA. This clearly results in a stepwise loss of alignment. One reason for this might be the progressive loss of hydrogen-bonding ability in the *N*-methyl derivatives that would prevent molecular aggregates or chains from forming. The increase in molecular size in the series would also be expected to have a large effect on the ability of the molecules to pack in an orderly way.

Other Hosts. SHG data: Complete SHG results for ALPO-5, SAPO-5, ALPO-11, and VPI-5 are shown in Table II. In marked contrast to ALPO-5 and SAPO-5, *ALPO-11 and VPI-5 align to some extent all of the organics tried.* The structural similarity between ALPO-5 and SAPO-5 result in the same pattern of SHG results for the various organics, that is, MNA is turned off, N-methylation shuts down the SHG in steps, NA and ANP

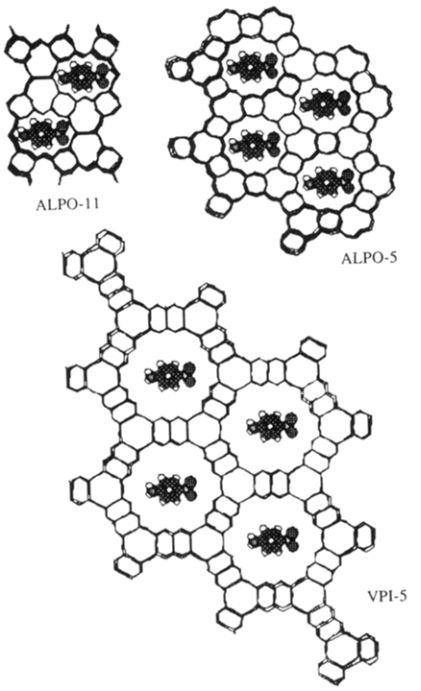

Figure 11. Cross-sectional views of ALPO-11, ALPO-5, and VPI-5.

are turned on, and ANPm and NPNO are not. The results for DMNA and NPNO in ALPO-11 and VPI-5 show that hydrogen bonding is not a necessary condition for alignment. Electrostatic interactions between host and guest and space restrictions within the channels must be enough to counteract the tendency of the molecular dipoles to pair up in opposite directions.

That NA (or ANP) is aligned by all three host structures is somewhat surprising because the three structures have such different space restrictions. This is demonstrated in Figure 11, which shows cross sections of the structures perpendicular to the channel axes with one NA molecule perpendicular to each channel. The ALPO-11 structure is clearly too small for NA to fit in this way, ALPO-5 looks borderline and, as noted above, is slightly too small, while VPI-5 has free space around the NA. These three structures could cause very different types of NA aggregation, but they also could all support the chain formation model presented above. Indirect evidence for a similar type of chain formation in ALPO-11, ALPO-5, and VPI-5 comes from the loading studies presented below.

UV–vis data: The color of many of the inclusion materials is significantly different than the pure organics. NA and its derivatives are solvatochromic; the lowest energy absorption band of NA moves from 320 nm in methylcyclohexane to 380 nm in *N*,*N*-dimethylformamide.[46]

Table III[a]

guest	pure cutoff	pure λ_{max}	in host ALPO-5[b] cutoff	ALPO-5[b] λ_{max}	SAPO-5[c] cutoff	SAPO-5[c] λ_{max}	ALPO-11[d] cutoff	ALPO-11[d] λ_{max}	VPI-5[e] cutoff	VPI-5[e] λ_{max}
NA	485	395	512	420	520	390	495	395	487	385
MNA	505	385	505	400	502	395	505	400	503	385
NMNA	512	420	545	420	545	410	522	410	507	405
DMNA	505	408	560	415	567	415	550	410	560	400
ANP	466	385	445	380	455	360	438	375	460	365
ANPm	410	350	410	350	410	335	400	350	412	346
NPNO	438	345	430	353	430	325	432	340	432	330

[a] Wavelengths in nanometers. All samples diluted 20–30% with magnesium carbonate. [b] 10–13 wt % guest loading level. [c] 12 wt % guest loading level. [d] 9–12 wt % guest loading level. [e] 20 wt % guest loading level.

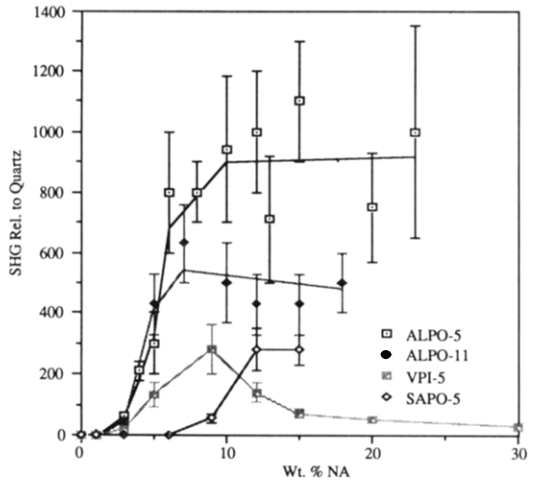

Figure 12. Relative SHG intensity versus wt % NA in ALPO-5, ALPO-11, VPI-5, and SAPO-5.

Diffuse reflectance UV–vis shows solventlike effects on the cutoff wavelength and absorption maximum in these samples compared to the pure organic. Broadening of the band is a general occurrence also. Data are shown in Table III and Figures 1–3 of the supplementary material (see the paragraph at the end of the paper). The NA absorption edge or cutoff wavelength is shifted by 30 nm in ALPO-5 and SAPO-5 but not shifted at all by VPI-5 and by only 10 nm by ALPO-11. MNA shows almost no shifts due to inclusion, but the *N*-methyl derivatives have large shifts of up to 60 nm. In ANP, ANPm, and NPNO the shifts are smaller but in the opposite direction. SAPO-5 and VPI-5 both depress the intensity of the lowest energy part of the band in all cases. This is very obvious for DMNA and NPNO but subtle for NA.

The mixing of ground and excited states is a major source of enhancement of the molecular second order susceptibility, β,[47] so that in general a lower energy electronic transition could contribute to increased SHG. All of the NA samples show large SHG intensities, but the band shift in ALPO-5 and SAPO-5 could be causing some SHG enhancement in these systems. No other obvious correlations between optical shifts and SHG are evident.

Variation of SHG with loading: The results of NA loading studies are shown in Figure 12. *ALPO-5 and ALPO-11 have a similar pattern of increasing SHG with loading* with an SHG threshold at about 3%. Data taken at JPL at 1.907 μm showed the same pattern. ALPO-11, with its smaller pore diameter, may therefore cause NA to form similar but stretched-out chains when compared to ALPO-5. This is shown schematically in Figure 13. From this figure it is evident that NA barely fits lengthwise into the ALPO-11 channel. How the larger methyl derivatives of NA (MNA, NMNA and DMNA) fit is unclear, and further modeling is underway.

VPI-5 shows a distinct maximum in SHG at about 9% NA, above which the SHG falls off. The much larger pores of VPI-5 must allow NA molecules to form molecular pairs with dipoles pointing in opposite directions. The maximum at intermediate loading fits well with a model where chains or aggregates of NA molecules similar to those present in ALPO-5 are forming without pair formation at intermediate loadings. Additional molecules can pair up with molecules already in a chain or form chains running in the opposite direction, causing the decrease in SHG. A

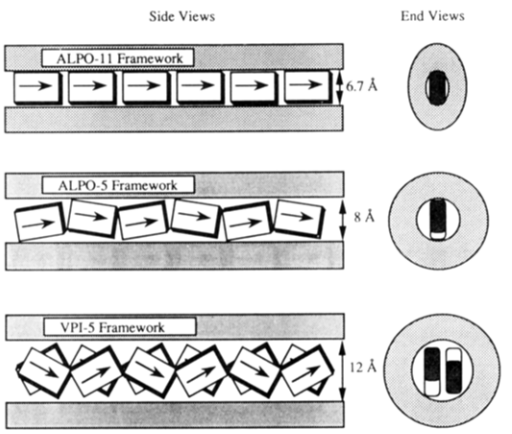

Figure 13. Models that show how NA molecules can fit into the channels of ALPO-11, ALPO-5 and VPI-5.

schematic representation of this idea is shown in Figure 13. Loading studies with larger organics, such as DMNA, which cannot form two parallel chains in VPI-5, are being undertaken to see if a similar maximum in SHG occurs.

Determination of unit cell expansion to establish that inclusion is occurring was attempted for ALPO-11 and VPI-5. No lines due to the pure organic phase were observed until loadings above 10% were reached. When taken under an inert atmosphere, X-ray diffraction of loaded VPI-5 showed a highly modified pattern that suggested new lattice crystallographies. The well-behaved example of ALPO-5 and the fact that SHG is observed in the NA-loaded samples are additional proof that the same kinds of inclusion phenomena are occuring in the other host systems.

SAPO-5 loading data present the first evidence that host framework charge or dielectric constant is an important parameter in these studies. Figure 12 shows that *the SHG threshold in SAPO-5 occurs at a much higher loading level than in ALPO-5*. NA molecules must be more strongly attracted to the charged SAPO-5 framework and/or extraframework cations than in ALPO-5, so that the intermolecular interactions are disrupted until a high enough loading is reached. One would predict that higher silicon contents in the SAPO-5 would eventually shut off all SHG. For NA at least, strong guest–host interactions are detrimental to SHG. This finding suggests a new type of conceptual nonlinear optic tuning effect in which *changes in host dielectric results in large variations in SHG* without changing guest concentration.

These last results show how important it is to carry out loading studies in systems showing the self-assembly of molecules. With only one data point, the SAPO-5 and VPI-5 systems seemed similar to ALPO-5. The loading studies clearly demonstrated the effects of framework charge and spatial restraints on molecular aggregation and alignment in molecular sieves.

Conclusions

Inclusion chemistry is a promising avenue for the development of new nonlinear optical materials. The first examples of organic guests in inorganic hosts that show large second-order optical nonlinearities have been described and examined. Twenty host–guest combinations show alignment of guest molecules as evidenced by SHG signals. They are composed of organics such as NA that are within the pores of the aluminophosphate hosts ALPO-11, ALPO-5, and VPI-5 and the silicoaluminophosphate SAPO-5. TGA results show that these materials exhibit enhanced thermal stability over the pure organic compounds.

(46) Khalil, O. S.; McGlynn, S. P. *J. Lumin.* **1975/76**, *11*, 185–196.
(47) Plugh, D.; Morley, J. O. In ref 1e, Chapter II-2, pp 193–225.

Weak intermolecular hydrogen bonding is an important factor for NA in ALPO-5 and may cause the self-assembly of molecular aggregates or chains that are aligned by the host channels. Similar aggregates may form in the other hosts. Structural work is in progress to further elucidate the alignment mechanism in these materials.

Three modes of SHG tuning are demonstrated by these materials: (1) variation in loading level, (2) variation in guest structure or composition, and (3) variation in host framework charge or dielectric constant. This allows great flexibility in formulating promising new combinations and shows that there are many avenues left to be explored. The systems are particularly important in providing the foundation for understanding the self-assembly of molecules and both inter- and intramolecular cluster interactions in supramolecular lattices. Molecular modeling studies of these properties are in progress.

Acknowledgment. The research support of the Office of Naval Research and E. I. Du Pont is gratefully acknowledged. We also thank Seth Marder, Albert Steagman, and Joe Perry of Jet Propulsion Laboratory for their advice and assistance in SHG measurements at 1.907 μm.

Supplementary Material Available: Diffuse reflectance UV–vis spectra of pure NA, pure DMNA, and pure NPNO at various concentrations in the various described molecular sieves (3 pages). Ordering information is given on any current masthead page.

Characterization of a Novolac-Based Three-Component Deep-UV Resist

Dennis R. McKean,* Scott A. MacDonald, Robert D. Johnson, Nicholas J. Clecak, and C. Grant Willson

IBM Research Division, Almaden Research Center, 650 Harry Road, San Jose, California 95120-6099

Received July 16, 1990

High-sensitivity positive-tone deep-UV resists are described that utilize acid-catalyzed chemistry in novolac resin. These resists are composed of an acid-sensitive dissolution inhibitor, an acid photogenerator, and novolac resin. The lithographic functioning and processing of these resists are very similar to the familiar diazonaphthoquinone/novolac systems but with nearly a 100-fold increase in sensitivity. The resist sensitivity shows a surprising dependency on the choice of casting solvent, and this effect has been demonstrated to be related to the resist chemistry, which has been studied by using ^2H NMR spectroscopy. The resist mechanism has been demonstrated to be primarily due to acid catalyzed thermolysis of the *tert*-butyl carbonate functional groups. The imaging characteristics of these resists is limited by the absorbance of the novolac resin, but submicron $[TTPFe^{IV}(C_6H_4CH_3\text{-}p)]^+$ has been obtained.

Introduction

Lithographic technology has advanced to the point that resolution capability well below 1 μm is now practiced in full-scale manufacturing of semiconductor devices. This may be achieved by use of high numerical aperture *i*-line or *g*-line step-and-repeat tools or by use of deep-UV lithography (200–300 nm). In the diffraction limit, the use of shorter wavelength radiation offers improved resolution and this has been demonstrated experimentally.[1,2] It now appears that use of deep-UV lithography may allow optical lithography to be extended well below 0.5-μm resolution. Deep-UV lithography has now been demonstrated by using commercial deep-UV lithographic tools that have both relatively broadband mercury emission sources and very narrow 248-nm excimer laser light sources. However, this has necessitated the development of new deep-UV resist materials since the traditional diazonaphthoquinone/novolac resists are inadequate for deep-UV lithography.[3,4]

Resist development for deep-UV lithography has evolved along several paths since the initial work with poly(methyl methacrylate) (PMMA).[1] PMMA resist functions by photoinduced cleavage of the polymer main chain that renders the exposed region of the polymer more soluble in certain developer solvents. Several other acrylate-type polymers are also sensitive in the deep-UV region as are isopropenyl ketone polymers.[5] In addition, negative deep-UV systems have been developed on the basis of the use of azide sensitizers that cross-link upon exposure to deep-UV radiation.[6]

All of these approaches however suffer from lack of sufficient sensitivity to deep-UV radiation. The exposure doses required to achieve reasonable throughput are considerably less for deep-UV lithography than for longer wavelengths. This appears to be true both for conventional mercury light sources and for excimer laser light sources. The higher sensitivity demand for deep-UV resists required the development of resists that were not limited by the quantum yield for the photochemical conversion.

High-sensitivity resists for deep-UV application have been developed around the concept known as chemical amplification, which separates the photochemical event from the bulk chemical change that is ultimately responsible for imaging.[7] This has been accomplished by ex-

(1) Lin, B. J. *J. Vac. Sci. Technol.* **1975**, *12*, 1317.
(2) Moreau, W. M.; Schmidt, R. R. *138th Electrochem. Soc. Meeting Extended Abstract* **1970**, 459.
(3) Iwayanagi, T.; Ueno, T.; Nonogaki, S.; Ito, H.; Willson, C. G. In *Electronic and Photonic Applications of Polymers*; Bowden, M. J., Turner, S. R., Eds.; American Chemical Society: Washington D.C., 1988; p 109.
(4) Sheats, J. R. *Solid State Technol.* **1989**, 79.
(5) Tsuda, M.; Oikawa, S.; Nakamura, Y.; Nagata, H.; Yokata, A.; Nakane, H.; Tsumori, T.; Nakane, Y.; Mifune, T. *Photogr. Sci. Eng.* **1979**, *23*, 290.
(6) Iwayanagi, T.; Kohashi, T.; Nonogaki, S.; Matsuzawa, T.; Douta, K.; Yanazawa, H. *IEEE Trans. Electron Devices* **1981**, *ED-28*, 1306.

0897-4756/90/2802-0619$02.50/0